Pergamon

Int. J. Heat Mass Transfer. Vol. 37, No. 18, pp. 2969–2984, 1994

0017–9310/94 $7.00+0.00

0017–9310(94)00114–6

A numerical study on natural convection of a heat-generating fluid in rectangular enclosures

A. G. CHURBANOV and P. N. VABISHCHEVICH†

Institute for Mathematical Modeling, Russian Academy of Sciences, 4 Miusskaya Square, Moscow 125047, Russia

and

V. V. CHUDANOV and V. F. STRIZHOV

Institute of Nuclear Safety, Russian Academy of Sciences, 52 B. Tulskaya, Moscow 113191, Russia

(*Received* 27 *December* 1993)

Abstract—Unsteady natural convection of a heat-generating fluid in the enclosures of a rectangular section with isothermal or adiabatic rigid walls is investigated numerically in the present work. Using the high-performance finite-difference scheme in the 2D stream function–vorticity formulation, developed by the authors, the peculiarities of convective heat transfer are studied in a wide range of thermal and geometric parameters for the laminar regime of fluid motion. Steady-state as well as oscillating solutions obtained in this work are compared with available numerical and experimental results of other researchers.

INTRODUCTION

Many problems of practical interest deal with buoyant flows in enclosures. Flows driven by temperature gradients have been studied extensively in many experimental and computational works. A comprehensive survey on this subject has been presented by Ostrach [1].

A more complicated situation, where there are volumetric energy sources in cavities with isothermal and/or adiabatic rigid walls, is also very important for applications. In the present work the peculiarities of laminar convective heat transfer in a heat-generating fluid layer are examined numerically with particular emphasis on nuclear reactor safety analysis. This problem has various formulations from the viewpoint of the geometry of the domain under consideration (cylindrical, hemispherical, horizontal layer, etc.) as well as in terms of imposed boundary conditions (isothermal or adiabatic). A comprehensive review of different formulations and the results obtained is presented in ref. [2]. Some preliminary results have been obtained by the authors of the present work for cylindrical and hemispherical enclosures [3]. In the present work this problem is considered for an enclosure of rectangular section with uniform isothermal or thermally insulated rigid walls. Such a formulation agrees with the measurement conditions [4–7], as well as with the formulation of numerical [8, 9] and combined numerical–experimental [10] works, which allow us to employ some of the results of these researches for the verification of the accuracy of the mathematical model used in our calculations and for the validation of the prediction reliability.

The urgency of the problem results from the necessity to predict correctly the behaviour of a molten heat-generating corium for various hypothetical accident scenarios in a pressurized water reactor (PWR). The situation where a molten corium flowed down to the bottom of a PWR vessel and buoyancy-driven corium flow occurred can be considered as an example of such scenarios. The accident at the Three Mile Island NPP in the U.S.A. developed in an approximately similar way.

GOVERNING EQUATIONS

Laminar natural convection of a heat-generating fluid with uniform volumetric energy sources is governed by an energy equation and unsteady Navier–Stokes equations with the Boussinesq approximation for buoyancy. In the temperature–vorticity–stream function formulation for the 2D case these equations can be written in the following dimensionless form:

$$\frac{\partial\theta}{\partial\tau}+\frac{\partial(u\theta)}{\partial x}+\frac{\partial(v\theta)}{\partial y}=\frac{1}{Pr}\left[\frac{\partial^2\theta}{\partial x^2}+\frac{\partial^2\theta}{\partial y^2}+1\right] \quad (1)$$

$$\frac{\partial\omega}{\partial\tau}+\frac{\partial(u\omega)}{\partial x}+\frac{\partial(v\omega)}{\partial y}=\frac{\partial^2\omega}{\partial x^2}+\frac{\partial^2\omega}{\partial y^2}+\frac{Ra}{Pr}\frac{\partial\theta}{\partial x} \quad (2)$$

† Author to whom correspondence should be addressed.

NOMENCLATURE

c_p specific heat [J kg^{-1} K^{-1}]
g gravitational acceleration [m s^{-2}]
H cavity height [m]
k thermal conductivity [W m^{-1} K^{-1}]
l tangential direction to a wall
L cavity length [m]
m isolines number
n normal direction to a wall
Nu local modified Nusselt number, $q_w/(sH) = -(\text{grad}\,\theta)_w$
$\overline{Nu}$ average Nusselt number [equation (8)]
Pr Prandtl number, ν/α
q_w local heat flux on the boundary surface, $-k(\text{grad}\,T)$ [W m^{-2}]
Ra modified Rayleigh number, $(g\beta sH^5)/(\alpha\nu k)$
s rate of volumetric heat generation [W m^{-3}]
T temperature [K]
T_w fixed temperature on the walls [K]
u dimensionless horizontal velocity, UH/ν
U horizontal velocity [m s^{-1}]
v dimensionless vertical velocity, VH/ν
V vertical velocity [m s^{-1}]
x dimensionless horizontal coordinate, X/H
X horizontal coordinate [m]
y dimensionless vertical coordinate, Y/H
Y vertical coordinate [m].

Greek symbols
α thermal diffusivity, $k/(\rho c_p)$ [m^2 s^{-1}]
β thermal expansion coefficient [K^{-1}]
θ dimensionless temperature, $(T-T_w)/(sH^2/k)$
ν kinematic viscosity [m^2 s^{-1}]
ρ density [kg m^{-3}]
τ dimensionless time, $t\nu/H^2$
ψ dimensionless stream function, $\Psi/(\nu H)$
Ψ stream function
ω dimensionless vorticity, $\Omega D^2/\nu$
Ω vorticity.

Subscripts
w wall
TOP top wall
LFT left wall.

$$\frac{\partial^2\psi}{\partial x^2}+\frac{\partial^2\psi}{\partial y^2}=-\omega \tag{3}$$

$$u=\frac{\partial\psi}{\partial y}\quad v=-\frac{\partial\psi}{\partial x} \tag{4}$$

where θ, ω, ψ, u and v stand for the dimensionless temperature, vorticity, stream function, horizontal and vertical velocity components, respectively; x, y are dimensionless Cartesian coordinates and τ is the dimensionless time. $Pr\,(\nu/\alpha)$ is the Prandtl number; $Ra\,[(g\beta sH^5)/(\alpha\nu k)]$ is the modified Rayleigh number, based not on the reference temperature difference but on the volumetric heat generation value, since the temperature difference is unknown *a priori* in this problem. Uniformly distributed internal heat sources are considered in the problem. Normalization is done here via the cavity height H, the kinematic viscosity ν and the value sH^2/k, proportional to a temperature difference. Three-dimensional and turbulent effects are neglected in this study.

A flow domain is an enclosed rectangular cavity with the fixed rigid walls and the following boundary conditions:

no-slip, no-permeability conditions for the velocity vector:

$$\psi=0\quad\frac{\partial\psi}{\partial n}=0 \tag{5}$$

isothermal or adiabatic thermal conditions:

$$\theta=0\quad\text{or}\quad\frac{\partial\theta}{\partial n}=0 \tag{6}$$

where n denotes the normal to the corresponding wall.

From equations (1)–(4) at prescribed boundary conditions and the aspect ratio we can obtain numerical solutions for various Rayleigh and Prandtl numbers. The quiescent state $\theta=\omega=\psi=0$ was used as the initial condition for the time integration in all predictions.

NUMERICAL METHOD

A common drawback of most commonly used numerical algorithms based on the stream function–vorticity formulation is an explicit evaluation of the vorticity on no-slip rigid walls that induces an essential restriction on a time-step [11]. To solve equations of convective heat transfer (1)–(4) with boundary conditions (5) and (6), a new efficient finite-difference technique [12, 13] has been developed and employed. Let us briefly discuss its primary merits. A new additive implicit difference scheme based on the operator-splitting technique [14, 15] has been developed and applied in the present study. Boundary values of the vorticity are calculated completely implicitly in this approach. The scheme is unconditionally stable for linearized equations, i.e. a time-step does not depend practically on a spatial grid and is evaluated only from the temporal accuracy constraint for the nonlinear

phenomena considered. Further, convective terms are approximated via special second-order formulae based on the central differences. By so doing, we can obtain accurate results on enough coarse grids. Finally, in our predictions we employ modern high-performance iterative solvers of preconditioned conjugate gradient type which have a very high convergence rate and are capable of solving equations without diagonal dominance. All these peculiarities of the numerical method provide the possibility of solving complex transient physical problems on personal computers such as an IBM AT 486. More details of this method are available in refs. [12, 13].

The uniform grid used in the calculations was 40×40 steps for $H/L = 1$ and increased in the horizontal direction in proportion to the increase in the size of the rectangular cavity in that direction. The sufficiency of grids employed in our predictions was validated via preliminary comparative calculations on more fine grids derived by means of dividing in two (for instance, 80×80 and 160×160 grids have been used in the grid validation procedure for a square cavity). Steady-state solutions (if they exist) have been obtained as a limit of a time-evolution process. The temporal accuracy of periodic solutions was verified on predictions with various time-steps.

RESULTS AND DISCUSSION

Free convection of a heat-generating fluid has been studied extensively in a great number of experimental [4–7] as well as numerical [8–10] works. Data presented in them have been used where it was possible to verify our mathematical model and numerical results. A comprehensive verifying and validation of our numerical method on the problems with internal heat sources as well as further parametrical investigations have been performed for rectangular enclosures in the following range of parameter values:

Rayleigh number: $10^5 \leqslant Ra \leqslant 10^8$;
aspect ratio: $0.25 \leqslant H/L \leqslant 1$.

The Prandtl number was fixed in all calculations at $Pr = 7$. Various thermal boundary conditions have been considered: the case with all isothermal walls; next, a configuration with isothermal horizontal and adiabatic side walls; finally, the variant with isothermal top and insulated other surfaces was investigated, too. The range of parameters considered in our predictions is very close to regimes studied experimentally in refs. [4, 6, 7, 10] for salt water heated by an alternating electric current.

At the beginning of this work a verification of the developed numerical method has been made on the basis of experimental and calculated data for the given class of problems. Detailed measurements [7] and calculations [9] form the basis for such a comparison. These results have been obtained for the cavity of square section (aspect ratio equals to 1) with all four rigid walls isothermal. It should be noted that the following relations take place due to some distinction in the normalization procedure: $Ra\ [7, 9] = Ra/64$, $\theta\ [7, 9] = 8\theta$ and $Nu\ [7, 9] = 4Nu$. The chosen range of Rayleigh numbers corresponds to laminar steady or unsteady periodical flow regimes.

The results of the calculations are given in Figs. 1–13 in the following form. Flow patterns and temperature fields are presented via streamlines and isotherms, respectively. The contour values are defined equidistantly between the function extremums as follows (for instance, for the stream function):

$$\psi_i = \psi_{\max} - (\psi_{\max} - \psi_{\min})/(m+1) \quad i = 1, m. \quad (7)$$

As a rule, the isolines number m was equal to 18 for the stream function and 8 for the temperature. As for the temporal histories of the heat transfer process, the plots show the maximum temperature $\theta_{\max}$ and the average Nusselt number $\overline{Nu}$ for the corresponding surface, defined as

$$\overline{Nu} = 1/L \int_0^L Nu \, dl \quad (8)$$

where l denotes the x- or y-coordinates along the corresponding wall.

Figure 1 presents the calculated steady-state regime for $Ra = 6.4 \times 10^5$. A fluid circulates in the square cavity as two symmetrical counter-rotating rolls, moving upward at the center of the cavity and downward near the cold side walls. Two local temperature maxima are shifted upward to the side walls.

As obtained in the previous works, the structure of thermal and hydrodynamic fields becomes more complicated with the increase in Rayleigh number to 3.2×10^6 (see Fig. 2). Two additional secondary vortices occur near the top wall, leading to the appearance of a downward-moving flow near the centerline in the vicinity of the upper surface. Such a change in the vertical velocity sign at the centerline in the upper part of the cavity for this Rayleigh number is confirmed by experimental [5, 7] as well as numerical [9] data. Due to the four-vortex structure of the flow, two local temperature maxima occur in the flow bulk and two thermal flux maxima appear at the upper surface. Moreover, the flow in such a regime becomes periodically oscillating, which can be clearly seen in our calculations. This fact has also been obtained by predictions [9], but has not been observed with measurements [7]. Instantaneous flow patterns and thermal fields are depicted in Fig. 2 for two moments of the period. One of them demonstrates a practically symmetric solution whereas the second shows that symmetry is disturbed in the vicinity of the upper surface due to shifting of secondary vortices in the upper part of the cavity.

Time variations of the temperature maximum and average Nusselt numbers through the top and left surfaces of the cavity for this Rayleigh number are shown in Fig. 3. A comparison with similar periodic results [9] demonstrates a good agreement in the character of oscillations, but our results provide a

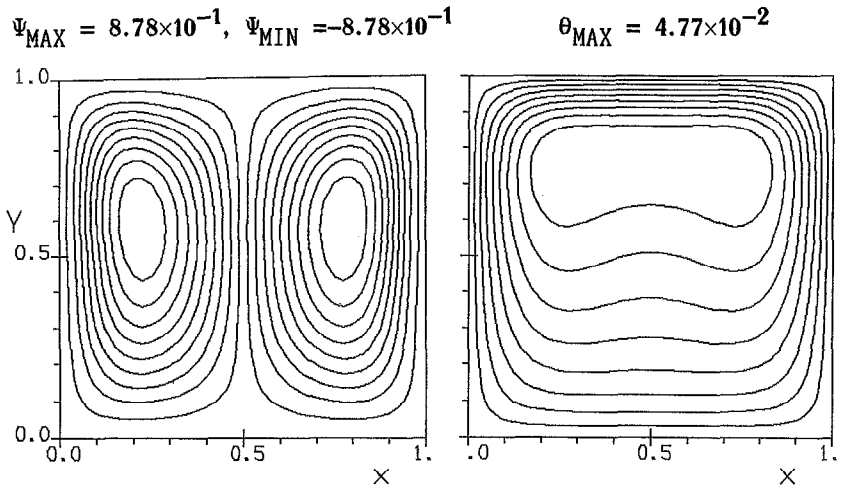

Fig. 1. Steady-state flow pattern and thermal field, $Ra = 6.4 \times 10^5$.

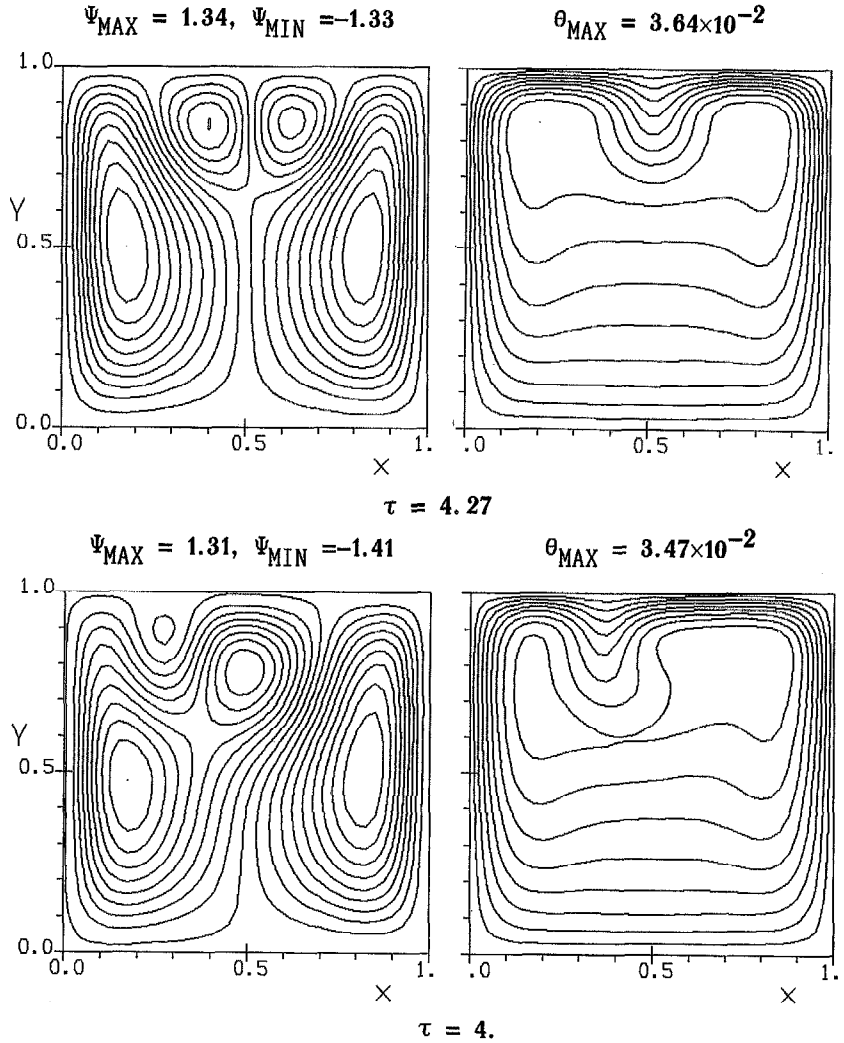

Fig. 2. Periodic oscillations, $Ra = 3.2 \times 10^6$.

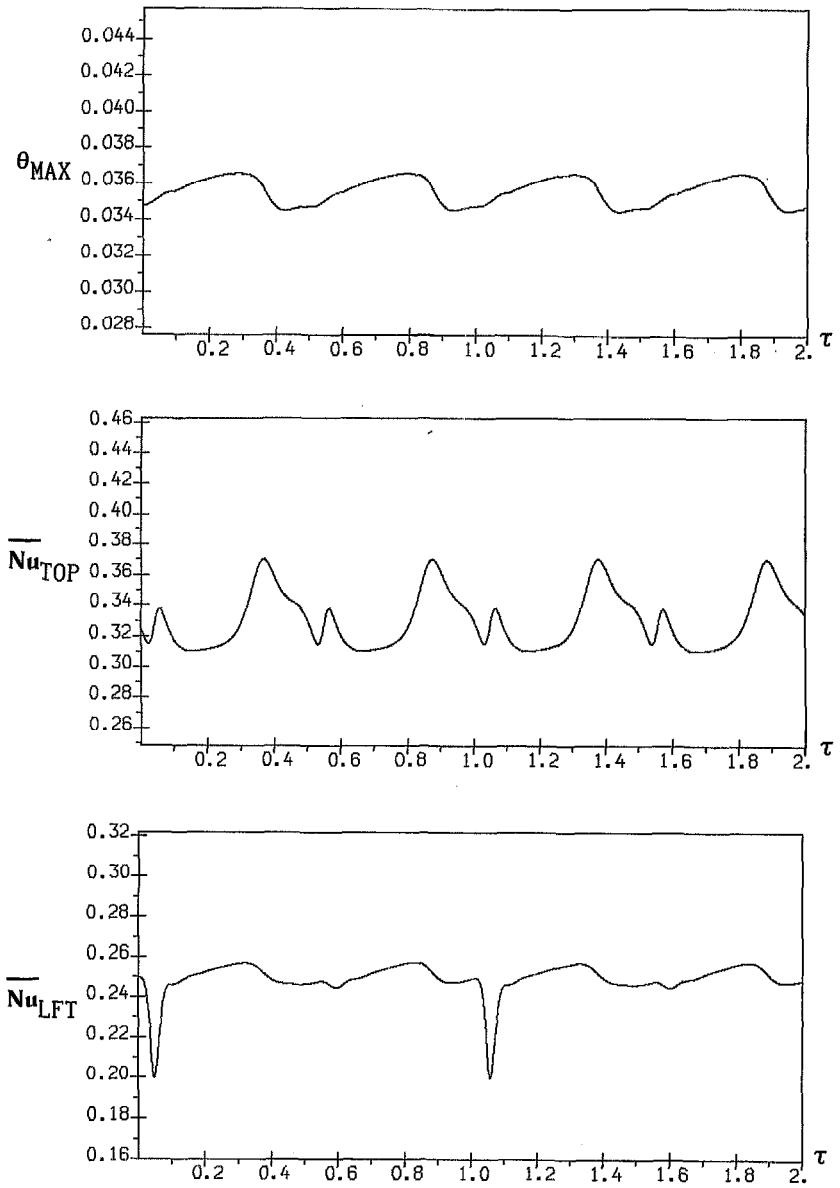

Fig. 3. Temperature maximum and $\overline{Nu}$ through the top and left surfaces vs time, $Ra = 3.2 \times 10^6$.

larger period value and a smaller oscillation amplitude. At the same time time-averaged values of θ_{max} obtained by our predictions are closer to experimental data (discrepancy less than 3%) than the above-mentioned calculations. It should be noted that, with increasing Rayleigh number, the value of θ_{max} is reduced.

Oscillations become more pronounced at higher Rayleigh numbers. Starting from $Ra = 10^8$ the flow becomes random fluctuating (see Fig. 4), which indicates a possible transition from the laminar to the turbulent regime. The range of Rayleigh number for the steady-state flow regime as well as for the periodic one were found to be practically the same as have been obtained numerically in ref. [2] for a hemispherical cavity of unit radius.

Similar results have been obtained for lower aspect ratio cavities, too. At low Rayleigh numbers the flow is also steady-state and shows a two-cell symmetric structure, but the values of the temperature maximum and average Nusselt numbers are higher compared to the square cavity. With increasing Rayleigh number periodical oscillations of all basic parameters occur again. At the same time, for both $H/L = 0.5$ and 0.25 the transition to periodic oscillations and random fluctuations occurs even at $Ra = 5 \times 10^5$ and 10^7, respectively, i.e. these two critical values of Rayleigh number are both lowered by a factor of approximately 10. The oscillating flow for $Ra = 5 \times 10^5$ and $H/L = 0.5$ is shown in Fig. 5. There are only two slightly-oscillating vortices in this case, which provides a practically constant θ_{max} but periodically varying

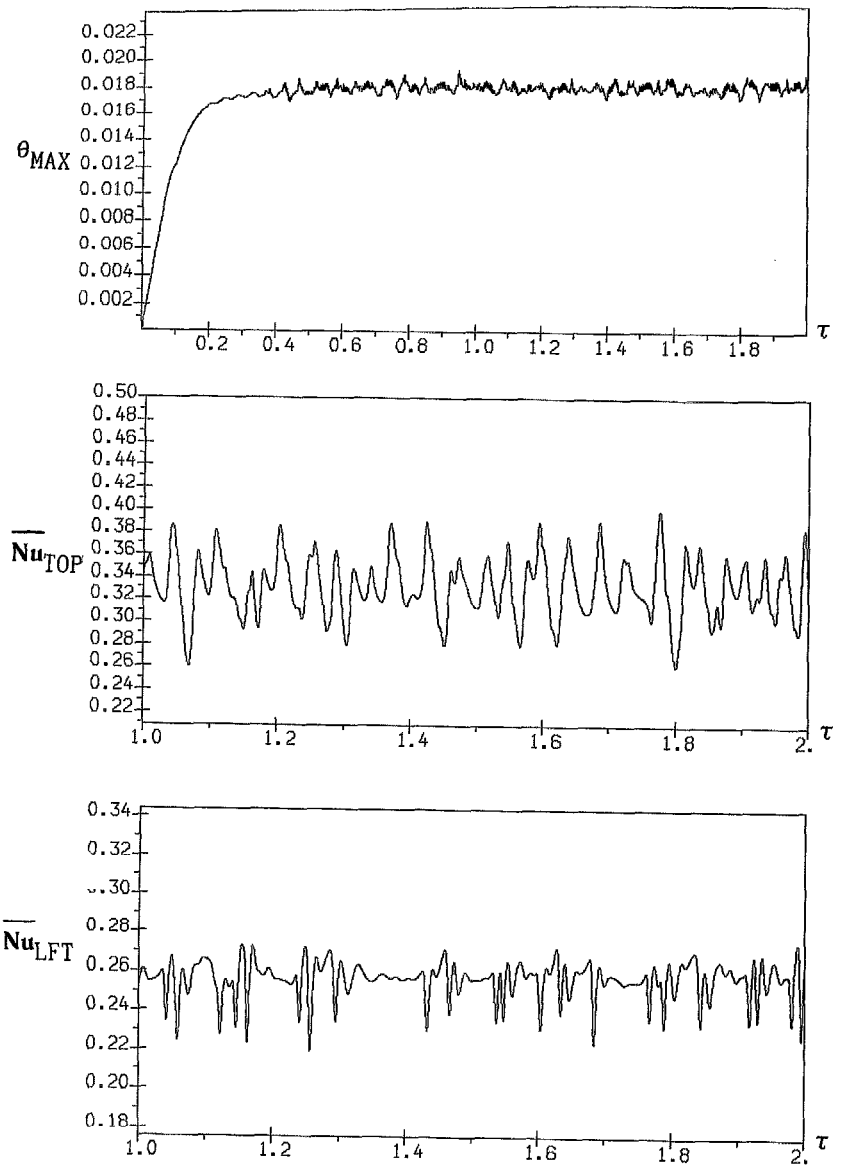

Fig. 4. Random fluctuating solution, $Ra = 10^8$.

average Nusselt numbers for the upper and left surfaces (see Fig. 6). At higher Ra values two main vortices break down into a multicellular structure due to a cavity low aspect ratio that is typical for free convection in thin layers. Figure 7 presents such a multicellular structure for the oscillating flow in the cavity with aspect ratio $H/L = 0.25$ and $Ra = 10^6$. The main tendency of the heat transfer evolution is conserved: with increasing Rayleigh number the average Nusselt number through the upper surface also increases but the maximum temperature value decreases.

The cases of two (side) and three (side and lower) adiabatic boundaries have also been studied for an aspect ratio equal to 0.5. The main regularity for both these formulations is the same as was found for the previous (isothermal) case with this aspect ratio, namely, starting from $Ra = 5 \times 10^5$ thermal and hydrodynamic fields become periodically oscillating, whereas the random fluctuation regime begins at $Ra \approx 10^7$. However, oscillations observed with these boundary conditions are much weaker.

The steady-state solution for the cavity with two thermally insulated sides at $Ra = 10^5$ is presented in Fig. 8. The solution is fundamentally different kind from the same regime with all boundaries isothermal (see Fig. 5 with similar Ra value for a comparison). There are already four vortices in this flow pattern. Moreover, the fluid circulates in the diametrically opposite direction: downward at the symmetry line

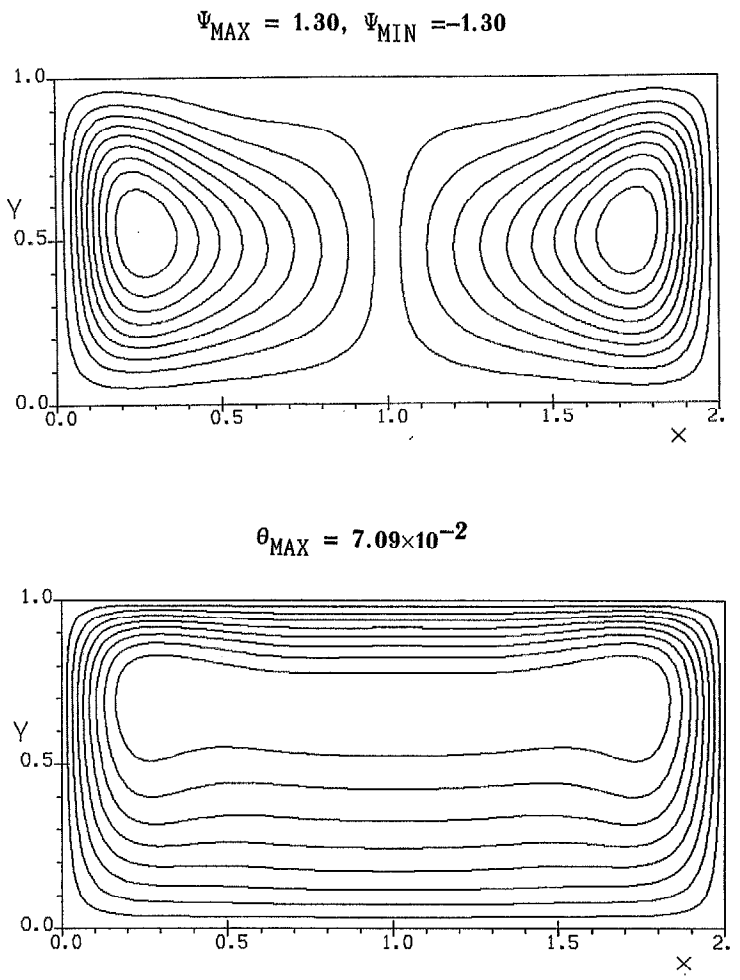

Fig. 5. Slightly-oscillating regime, $Ra = 5 \times 10^5$.

and upward between large and small rolls (it is clearly visible from the isotherm structure). Very weak oscillations occur at $Ra = 5 \times 10^5$, i.e. the solution is practically quasi-steady with the structure depicted in Fig. 9. This prediction is in a good agreement with data for computational and real experiments [10] obtained for $Ra = 7 \times 10^5$. Only at $Ra = 10^6$ do oscillations become more pronounced (see Figs. 10 and 11) due to the fact that convective motion is decomposed into evolving vortical cells of different size.

It was found that a further change in thermal conditions at the bottom into adiabatic ones slightly smooths the spatial nonuniformity of the hydrodynamical field (decreases the number of vortices), but as a whole it does not affect considerably the main features of convective heat transfer. A typical solution for this problem is depicted in Figs. 12 and 13 for $Ra = 10^6$. Obviously, a further reduction in oscillation amplitude takes place for thermal parameters in this flow regime compared to similar predictions with two adiabatic sides (see Figs. 10 and 11).

CONCLUSIONS

A new numerical algorithm developed by the authors to solve convective heat transfer problems demonstrates high accuracy and efficiency properties when applied to problems with internal heat generation. A comprehensive comparison with numerical and experimental results of various authors indicates that with the help of this method it is possible to obtain correct numerical results for this very important class of thermal problems. New temporal and spatial dependencies of heat transfer are obtained on the basis of this method for a rectangular cavity with a heat-generating fluid in a wide range of thermal and geometric parameters. For various aspect ratios ranges of Rayleigh number are obtained for steady-state and

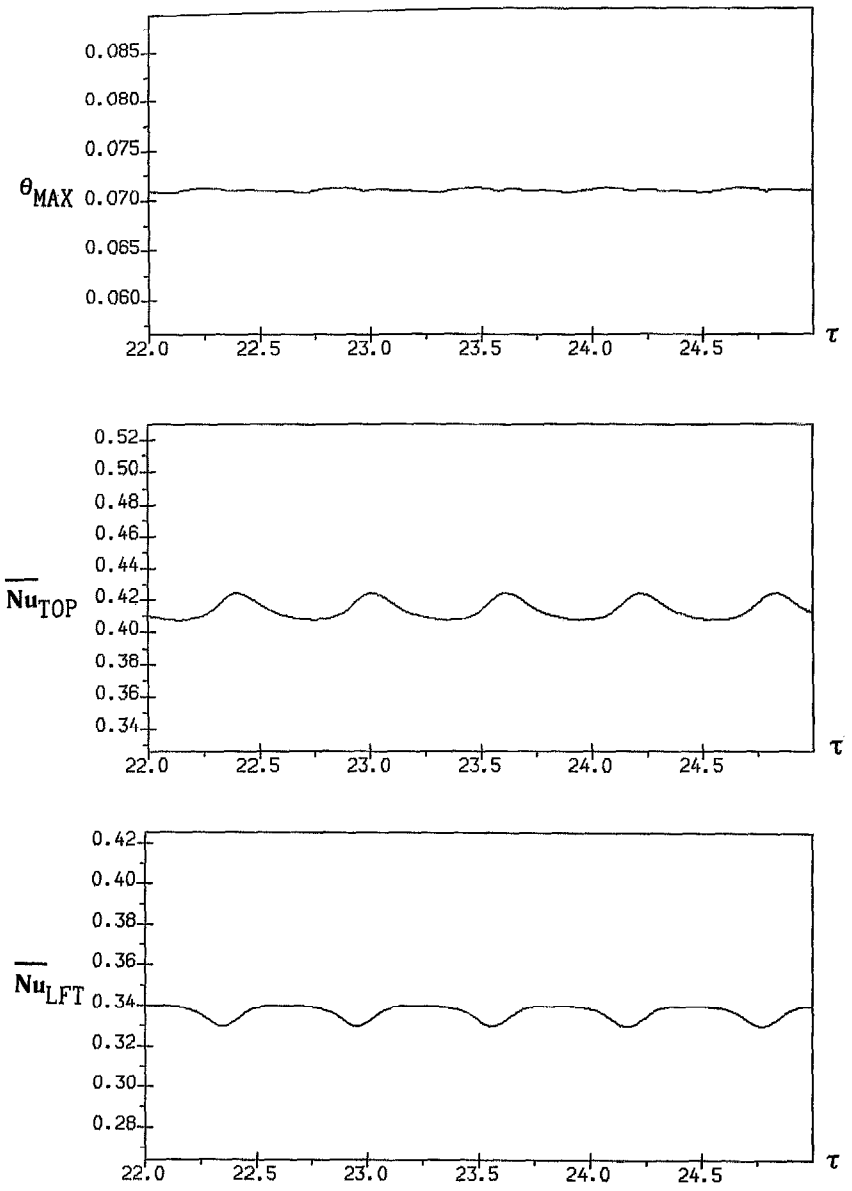

Fig. 6. Temporal variations of thermal parameters, $Ra = 5 \times 10^5$.

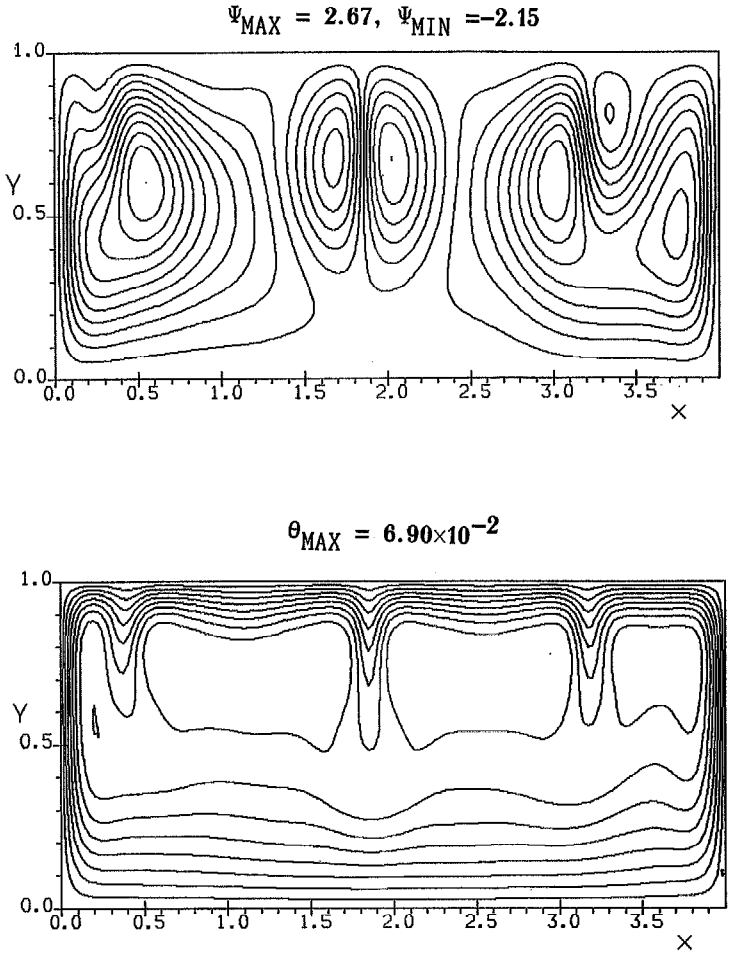

Fig. 7. Multicellular oscillating regime, $Ra = 10^6$.

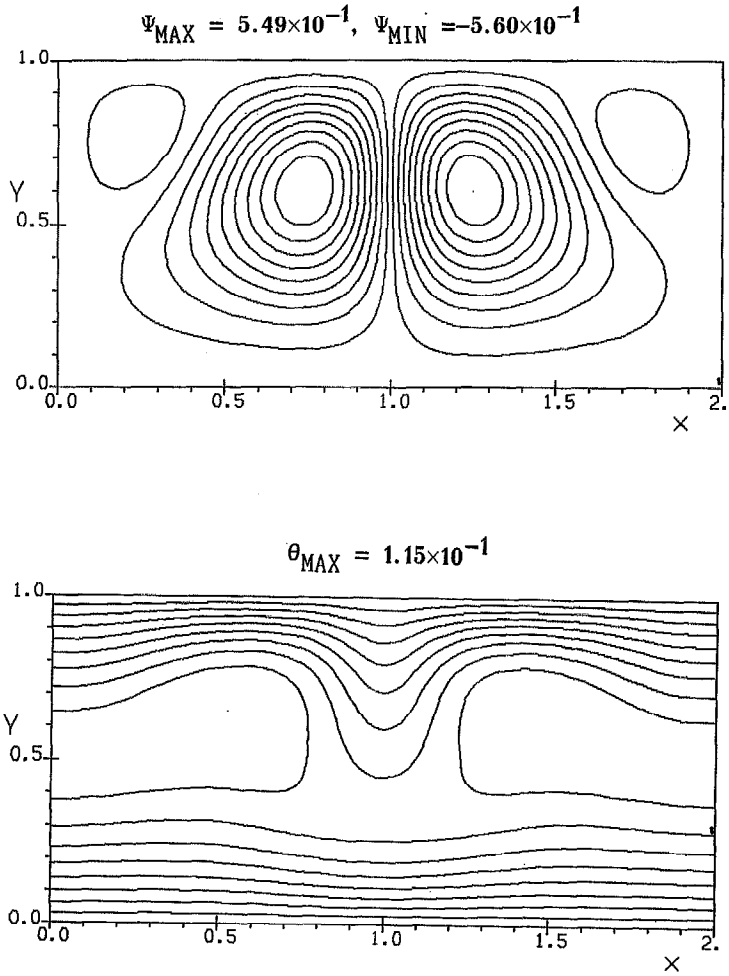

Fig. 8. Steady-state solution for adiabatic sides, $Ra = 10^5$.

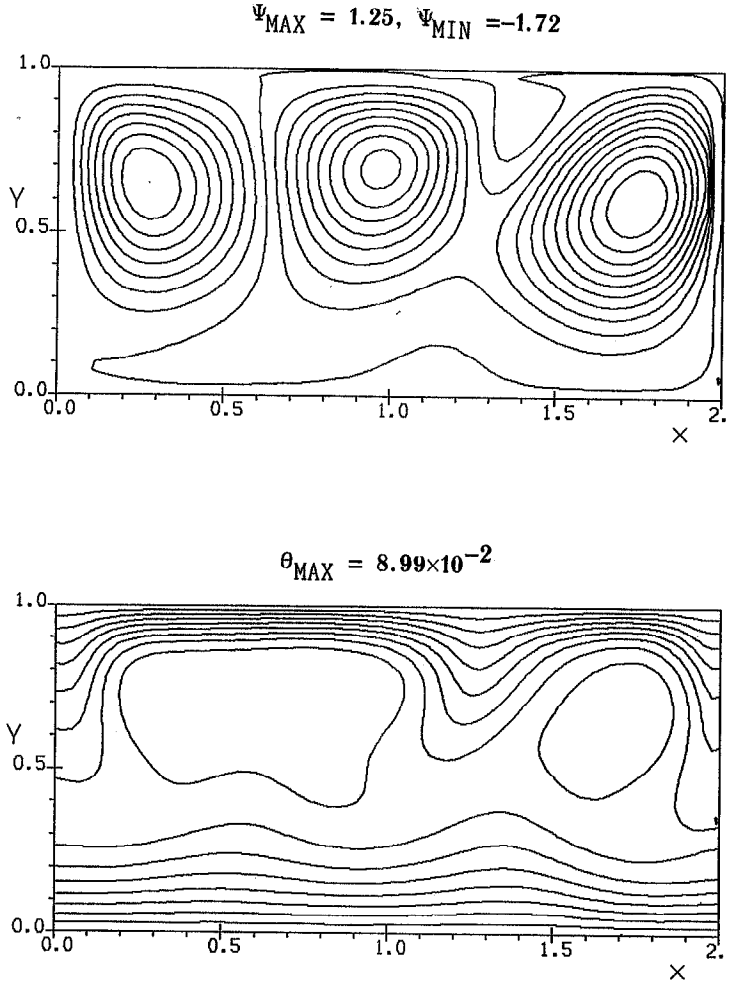

Fig. 9. Weak oscillations, $Ra = 5 \times 10^5$.

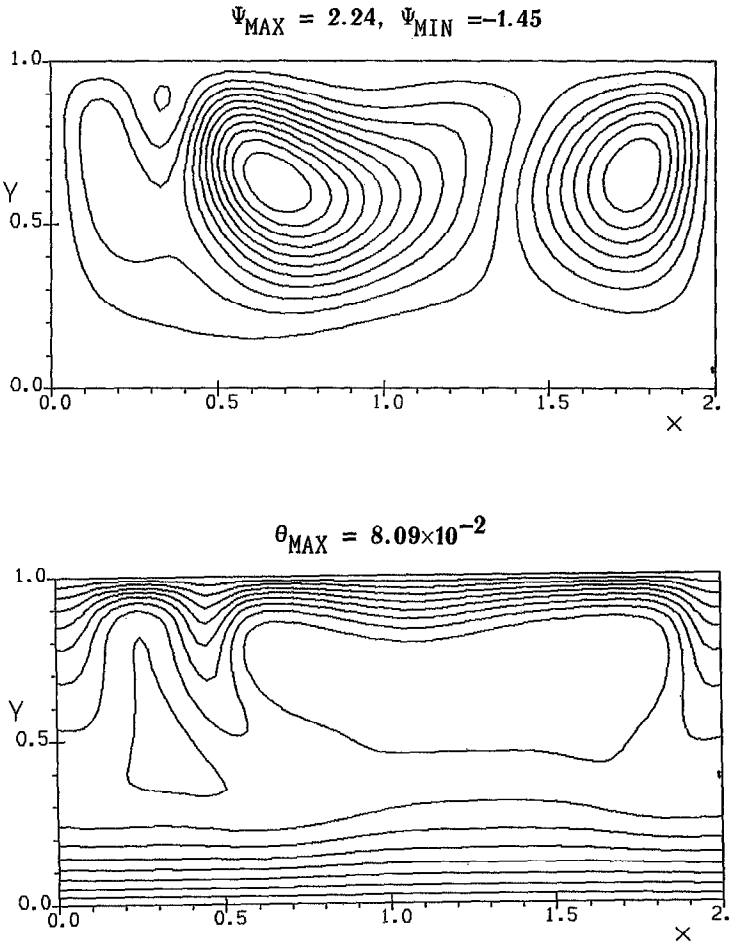

Fig. 10. Oscillating heat and fluid flow, $Ra = 10^6$.

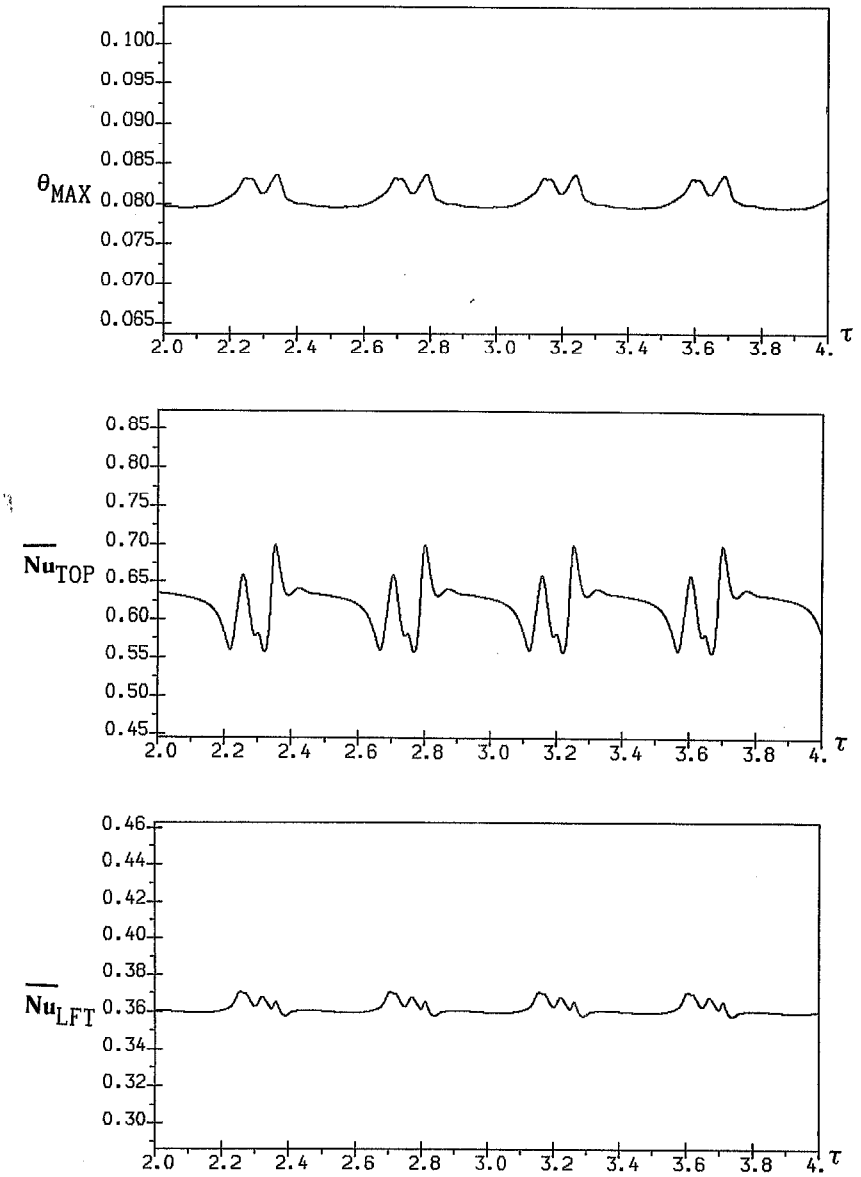

Fig. 11. Time variations of heat transfer, $Ra = 10^6$.

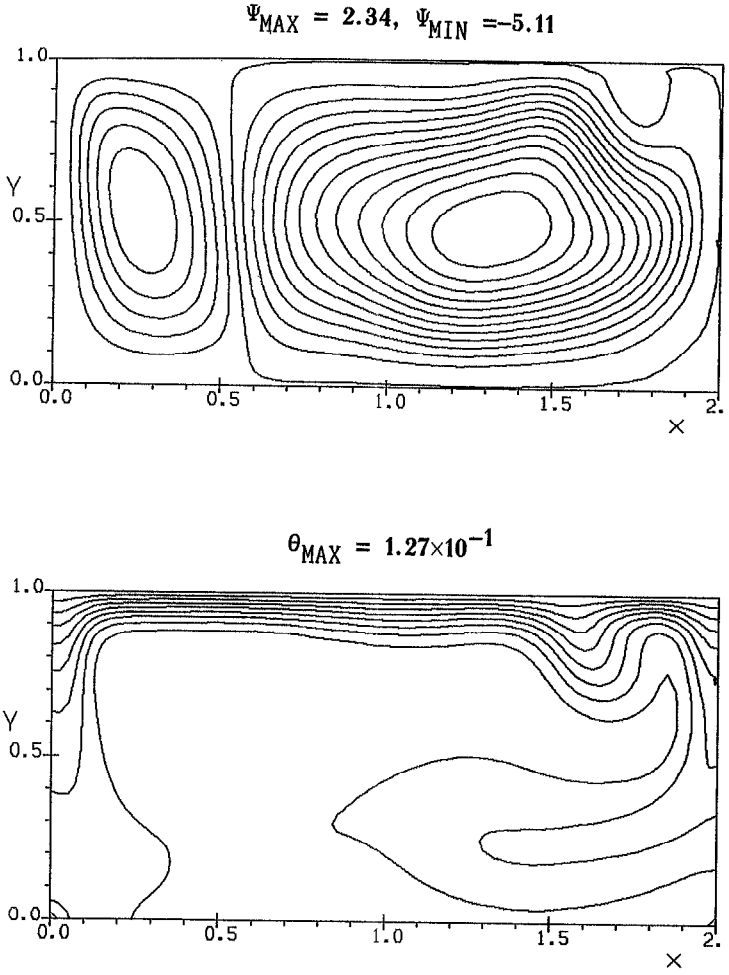

Fig. 12. Oscillations for adiabatic sides and bottom, $Ra = 10^6$.

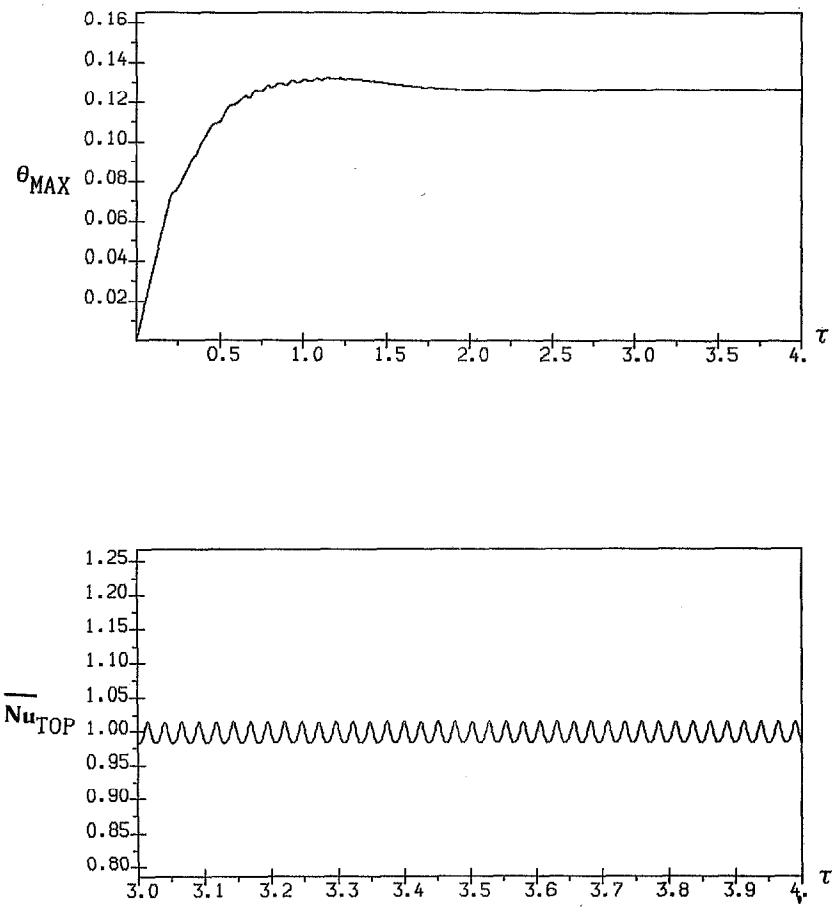

Fig. 13. Histories of the heat transfer process, $Ra = 10^6$.

oscillating flow regimes. It was found that flow in a square cavity becomes periodically oscillating at $Ra = 3.2 \times 10^6$ and random fluctuating at $Ra = 10^8$, respectively. On decreasing aspect ratio to 0.25 the critical Rayleigh numbers corresponding to the transition to the periodical regime as well as the random fluctuation are both reduced by a factor approximately of 10. A change of boundary conditions at the sides and bottom from isothermal to adiabatic leads to some depression of the oscillation amplitudes, but gives the same ranges of the Rayleigh number for steady and periodic regimes.

Acknowledgement—The authors are grateful to Dr A. G. Popkov for helpful discussions.

REFERENCES

1. S. Ostrach, Natural convection in enclosures, *ASME J. Heat Transfer* **110,** 1175–1190 (1988).
2. K. M. Kelkar, R. C. Schmidt and S. V. Patankar, Numerical analysis of laminar natural convection of an internally heated fluid in a hemispherical cavity, *Proceedings of National Heat Transfer Conference*, pp. 355–364. San Diego, CA (1992).
3. L. A. Bolshov, R. V. Arutyunyan, A. G. Popkov, V. V. Chudanov, P. N. Vabishchevich and A. G. Churbanov, Numerical study of natural convection of a heat-generating fluid in nuclear reactor safety problems, Submitted to the 4th International Topical Meeting on Nuclear Thermal Hydraulics, Operations and Safety, 5–8 April 1994, Taipei.
4. F. A. Kulacki and R. J. Goldstein, Thermal convection in a horizontal fluid layer with uniform volumetric energy sources, *J. Fluid Mech.* **55,** 271–287 (1972).
5. R. Farhadieh and R. S. Tankin, Interferometric study of two-dimensional Benard convection cells, *J. Fluid Mech.* **66,** 739–752 (1974).
6. F. A. Kulacki and A. A. Emara, Steady and transient thermal convection in a fluid layer with uniform volumetric energy sources, *J. Fluid Mech.* **83,** 375–395 (1977).
7. J.-H. Lee and R. J. Golstein, An experimental study on natural convection heat transfer in an inclined square enclosure containing internal energy sources, *ASME J. Heat Transfer* **110,** 345–349 (1988).
8. A. A. Emara and F. A. Kulacki, A numerical investigation of thermal convection in a heat-generating fluid layer, *ASME J. Heat Transfer* **102,** 531–537 (1980).
9. H.-O. May, A numerical study on natural convection in an inclined square enclosure containing internal heat sources, *Int. J. Heat Mass Transfer* **34,** 919–928 (1991).
10. M. Jahn and H. H. Reineke, Free convection heat transfer with internal heat sources: calculations and measurements. *Proceedings of 5th International Heat Transfer Conference*, pp. 74–78. Tokyo (1974).
11. P. J. Roache, *Computational Fluid Dynamics*. Hermosa, Albuquerque, NM (1976).
12. P. N. Vabishchevich, M. M. Makarov, A. G. Popkov, V. V. Chudanov and A. G. Churbanov, Numerical solution of hydrodynamics problems in the stream function-vorticity formulation. Preprint of Institute for Mathematical Modeling, Russian Academy of Sciences No. 22, Moscow (1993) (in Russian).
13. P. N. Vabishchevich, M. M. Makarov, V. V. Chudanov and A. G. Churbanov, Numerical simulation of convective flows in the stream function-vorticity-temperature formulation, Preprint of Institute for Mathematical Modeling, Russian Academy of Sciences No. 28, Moscow (1993) (in Russian).
14. A. A. Samarskii, *Theory of Difference Schemes*. Nauka Publishers, Moscow (1989) (in Russian).
15. G. I. Marchuk, *Methods of Numerical Mathematics*. Springer, New York (1975).